arXiv:cond-mat/0309545v1 [cond-mat.supr-con] 24 Sep 2003

Point-Contact Spectroscopy in MgB_2: from Fundamental Physics to Thin-Film Characterization

R.S. Gonnelli †[+], D. Daghero †, A. Calzolari †, G.A. Ummarino †, V. Dellarocca †, V.A. Stepanov ‡, S.M. Kazakov §, J. Karpinski §, C. Portesi ‖, E. Monticone ‖, V. Ferrando ¶ and C. Ferdeghini ¶

†INFM – Dipartimento di Fisica, Politecnico di Torino, 10129 Torino, Italy
‡P.N. Lebedev Physical Institute, Russian Academy of Sciences, 119991 Moscow, Russia
§Solid State Physics Laboratory, ETH, CH-8093 Zürich, Switzerland
‖ Istituto Elettrotecnico Nazionale "Galileo Ferraris", 10135 Torino, Italy
¶ INFM-LAMIA and Dipart. di Fisica, Università di Genova, 16146 Genova

Abstract. In this paper we highlight the advantages of using point-contact spectroscopy (PCS) in multigap superconductors like MgB_2, both as a fundamental research tool and as a non-destructive diagnostic technique for the optimization of thin-film characteristics. We first present some results of crucial fundamental interest obtained by directional PCS in MgB_2 single crystals, for example the temperature dependence of the gaps and of the critical fields and the effect of a magnetic field on the gap amplitudes. Then, we show how PCS can provide useful information about the surface properties of MgB_2 thin films (e.g. T_c, gap amplitude(s), clean or dirty-limit conditions) in view of their optimization for the fabrication of tunnel and Josephson junctions for applications in superconducting electronics.

1. Introduction

From the point of view of fundamental physics, magnesium diboride (MgB_2, discovered to be superconducting below 39 K in 2001 [1]) is particularly interesting because it is the clearest example of two-band superconductor ever studied [2, 3, 4]. However, this simple compound is also interesting because of its possible applications, that could take advantage of its rather low production cost and of its rather high T_c. At present, one of the most promising fields of application is superconducting electronics, with the perspective of MgB_2-based devices with good performances operating at a temperature ($\sim$ 10-15 K) accessible to one-stage cryocoolers. After the early observation of the Josephson effect in MgB_2 break junctions [5], the efforts in this directions have led to the fabrication of various kinds of Josephson and tunnel junctions [6] as well as prototypal SQUIDs [7].

Point-contact spectroscopy (PCS) has proved particularly useful in the fundamental research on MgB_2, since it allows measuring in a direct way both the gaps of this compound [8] with great accuracy [9]. Actually, being a surface-sensitive probe, PCS is also a unique experimental technique to study the surface superconducting properties of the material. Thus, we also used it as a diagnostic tool within a process of optimization of MgB_2 thin films, in view of the fabrication of Josephson junctions of different kinds and, finally, of simple superconducting electronic devices (e.g. SQUIDs).

In this paper we will first present some results of relevant fundamental interest we obtained by directional PCS in MgB_2 single crystals in the presence of magnetic fields up to 9 T, among which the temperature dependence of the critical field for $\mathbf{B} \parallel c$ and $\mathbf{B} \parallel ab$, and the temperature and magnetic-field dependence of the gap amplitudes. We will show how these results address some important subjects of present debate in the fundamental physics of MgB_2. Then, we will report the results of PCS measurements in MgB_2 thin films grown by different techniques on various substrates. These measurements provide information (e.g. about film orientation) that can be compared to structural and morphological results, such as XRD and AFM/STM. We will also show that PCS can give very useful indications about the conditions

[+] To whom correspondence should be addressed (renato.gonnelli@polito.it)

of the very surface (e.g., presence and effectiveness of impurities, oxidation, degradation) that are of crucial importance for the fabrication of tunnel and Josephson junctions for electronic applications, but *cannot* be provided by bulk-sensitive techniques.

2. Experimental details

2.1. The samples

The state-of-the-art MgB_2 single crystals used in our experiments were produced by J. Karpinski's group at the Solid State Physics Laboratory of ETH, Zurich (Switzerland). The crystal growth procedure occurs under a pressure of 30-35 kbar and is described in detail elsewhere (see for example Ref. [10]). For our purposes, we had to use crystals with regular shape (i.e. flat upper surface and sharp edges) even if they were rather small ($0.6 \times 0.6 \times 0.06\,\mathrm{mm}^3$ at most).

The thin films were produced either at the National Electrotechnical Institute (IEN) "Galileo Ferraris" in Turin (Italy) or at the LAMIA Laboratory of the National Institute for the Physics of Matter (INFM), in Genoa (Italy). Films on *c*-cut sapphire and MgO (111) (both with hexagonal surface symmetry, similar to that of MgB_2) were produced by using a two-step procedure by the Genoa group [11]. The first step consists in the PLD deposition of an amorphous, non-superconducting precursor layer in UHV (10^{-9} mbar) at room temperature, starting from a stoichiometric MgB_2 sintered target. The second step is an ex-situ annealing process in magnesium atmosphere, necessary to crystallize the superconducting phase. The samples are sealed in tantalum crucibles under Ar pressure with Mg lumps, closed in an evacuated quartz tube and kept at 850°C for half an hour with a following rapid quenching to room temperature. In addition to sapphire, the group from Turin also used amorphous silicon nitride (SiN) as substrate, which is particularly advantageous in view of the fabrication of bolometers [12]. The 500 nm-thick, amorphous SiN layer is grown on silicon wafer by LPCVD. The MgB_2 films are then deposited by simultaneous evaporation of Mg and B at constant temperature in a pressure of $5{\cdot}10^{-7}$ mbar from a Mo resistive heater and from a Mo crucible by e-beam heating, respectively. The resulting precursor is annealed *in situ* (i.e. in the deposition chamber) in Ar atmosphere, at 500°C. The resulting films look golden-brownish and mirror-like, are always very homogeneous and cover the whole surface of the substrates (about 5 cm^2).

2.2. Directional PCS in single crystals

As described elsewhere [9], the point contacts (of about $50 \times 50\,\mu\mathrm{m}^2$) were made by using a small piece of indium or a drop of Ag conductive paint. This ensured better mechanical stability on thermal cycling and reproducibility of the conductance curves with respect to the standard technique that employs a metallic tip pressed against the sample. The contacts were placed either on the top surface or on the side of the crystals, so as to inject the current mainly along the *c* axis or along the *ab* planes, respectively *.

Knowing the direction of current injection is important because of the anisotropy of MgB_2. In fact, PCS gives the $I-V$ characteristics and the conductance curves ($\mathrm{d}I/\mathrm{d}V$ vs. V) of a normal metal/superconductor junction. In the case of MgB_2, the conductance across such a junction contains (separate) contributions of the σ and π bands [3, 9]. Since the σ bands are almost 2D (and originate from the overlapping of in-plane sp^2 boron orbitals), their contribution to the conductance is maximum for current flowing along the *ab* planes. This is thus the most favorable configuration to observe clearly the σ-band gap together with the π-band one. The use of MgB_2 single crystals allowed us to perform these measurements and to test the predictions of the two-band model concerning the amplitudes of the gaps, their temperature- and magnetic field-dependency, and the relative weight of the two bands for *ab*-plane and *c*-axis current injection.

* Actually, the current is injected within a cone whose angle ϕ depends on the potential barrier at the interface: $\phi \to 0$ for tunneling ($Z \to \infty$) and $\phi = \pi/2$ for metallic contact with no barrier ($Z = 0$). Our contacts are always in an intermediate case, but the probability for electrons to be injected along an angle φ in the cone is proportional to $\cos\varphi$ [13] so that it is maximum along the normal direction anyway.

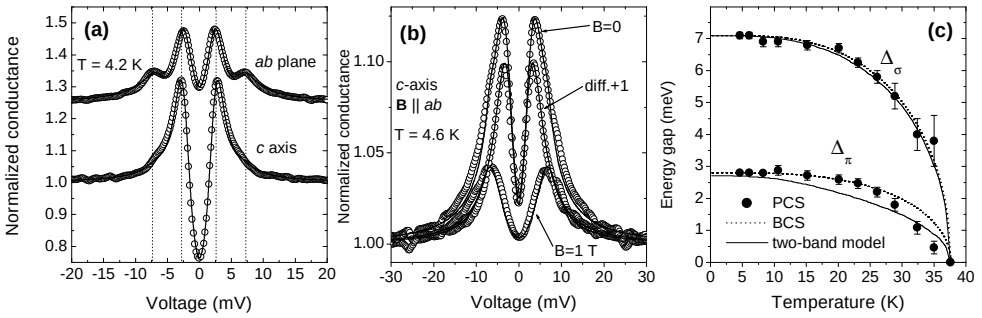

Figure 1. Some experimental results of directional PCS in MgB_2 single crystals. (a) Typical normalized conductance curves of a *ab*-plane and of a *c*-axis contact. Symbols: experimental data. Lines: best-fitting curves (two-band BTK model). (b) Symbols: experimental normalized conductance curves of a *c*-axis In contact, measured at 4.6 K in zero field ("B=0") and in the presence of a field of 1 Tesla ("B=1T"), together with the difference between these two, vertically shifted by 1 for best comparison ("diff.+1"). Solid lines: best-fitting curves obtained by using the functions $\sigma_{B=0}$, $\sigma_{B=1T}$ and $\sigma_{diff}+1$ defined in the text. (c) Temperature dependence of the gaps Δ_σ and Δ_π obtained from the fit of the partial σ- and π-band conductances (symbols). Dotted lines: BCS-like $\Delta(T)$ curves. Solid lines: predictions of the two-band model in the Eliashberg formulation [3].

2.3. PCS in thin films

As in single crystals, point contacts on films were made either by using a spot of Ag paint or a piece of indium placed on the top surface [+]. In this case, the weight of the σ-band contribution to the total normalized conductance is an indicator of the film orientation. For perfectly *c*-axis oriented films an almost pure *c*-axis conductance is expected, with little or no traces of the σ-band gap (as an example, see the lower curve in Figure1a). However, even in highly oriented films the σ-band contribution could be greater than expected if the surface roughness is not small enough, since microcontacts could be established also on the edge of grains or mesas. Similarly, even in films with very flat surface (such as those grown by hybrid physical-chemical vapour deposition (HPCVD) [14]) conventional PCS can give an excess σ-band contribution due to the partial penetration of the tip in the films. Probably, this explains the recent results by Bugoslavskij and coworkers [15].

In addition to the information about film orientation, PCS also provides information about possible enhancements or reductions of the superconducting properties at the surface the clean- or dirty-limit conditions at the surface (i.e., roughly speaking, the effectiveness of interband scattering due to impurities) and the existence of a degraded insulating layer, for example of MgO (which can arise from the reaction with atmosphere).

3. Results and discussion

3.1. Directional PCS in single crystals

Figure 1 reports some results of PCS in single crystals. In panel (a) symbols represent typical conductance curves of *ab*-plane and *c*-axis contacts. In the first case (upper curve) four conductance peaks are present, at $V \simeq \pm 2.8$ mV and $V \simeq \pm 7.6$ mV. These features are connected to the two gaps, Δ_π and Δ_σ. In *c*-axis contacts (lower curve) at the same voltages we observe clearly defined maxima and smooth shoulders, respectively. Such a difference is due to the aforementioned anisotropy of the σ bands, whose contribution to the conductance is minimum for *c*-axis current. That this contribution is not zero is clearly shown by the fact that the standard *s*-wave, single-band Blonder-Tinkham-Klapwijk (BTK) model [16] is not able to fit the conductance curves. On the contrary, the same model generalised to the two-band case, where the total *normalized* conductance is $\sigma = w_\pi \sigma_\pi + (1 - w_\pi)\sigma_\sigma$, gives rather good

[+] Note that the conventional PCS technique using a metallic tip could be unadvisable in this case, due to the risk of cracks in the film itself.

results (solid lines). The best fit is obtained with values of the gaps and of the weight w_π [9] that agree very well with the predictions of the two-band model in the Eliashberg formulation [3]. However, the accuracy of these values is rather poor since the fitting function contains 7 adjustable parameters: Δ_σ and Δ_π, the broadening parameters Γ_σ and Γ_π (that account for pair-breaking effects), the barrier transparency coefficients Z_σ and Z_π (proportional to the potential barrier height), and w_π.

Figure 1b illustrates the procedure we used to improve this accuracy [9]. Symbols represent the experimental normalized conductance curves of a *c*-axis In contact, measured in zero field ("B=0") and in the presence of a field of 1 Tesla ("B=1T"), together with the difference between these two, vertically shifted by 1 for best comparison ("diff.+1"). As discussed elsewhere [9, 17], the π-band contribution to the experimental conductance is strongly suppressed by the field and, at $B \simeq 1$ T, it is no longer detectable by our fitting procedure, while the σ-band gap remains practically unchanged. Thus, the conductance curve measured in a field of 1 T practically contains the σ-band conductance alone. If the conductance in zero field is given by $\sigma_{B=0} = w_\pi\sigma_\pi + (1-w_\pi)\sigma_\sigma$, the curve measured in $B = 1$ T is obtained by putting $\sigma_\pi = 1$ and thus has the functional form $\sigma_{B=1T} = w_\pi + (1-w_\pi)\sigma_\sigma$. Consequently, the difference between the two curves is expressed by $\sigma_{diff} = \sigma_{B=0} - \sigma_{B=1T} = w_\pi(\sigma_\pi - 1)$ and only contains the π-band contribution.

Fitting the experimental curves reported in the figure (symbols) with the corresponding functions $\sigma_{B=0}$, $\sigma_{B=1T}$ and σ_{diff} gives indeed very good results. The fitting curves are reported in Figure1b as solid lines. The best-fitting parameters are: $\Delta_\sigma = 7.1 \pm 0.1$ meV, $\Gamma_\sigma = 1.7$ meV, $Z_\sigma = 0.6$ from the fit of the curve in magnetic field; $\Delta_\pi = 2.80 \pm 0.05$ meV, $\Gamma_\pi = 2.0$ meV, $Z_\pi = 0.6$ from the fit of the difference. The clear advantage of this procedure, that allows separating the partial σ- and π-band conductances, is that the number of free parameters in each fitting function is reduced to three (w_π is fixed to the value one gets from the fit of $\sigma_{B=0}$, i.e., in the case of Figure 1b, $w_\pi = 0.98$) with a consequent reduction of the uncertainty on the gap amplitudes.

If this procedure is repeated at any temperature, one obtains the complete temperature dependence of the gaps reported in Figure 1c (symbols). Two BCS-like curves (dots) and the $\Delta_{\sigma,\pi}(T)$ curves predicted by the two-band model [3] (solid lines) are reported for comparison. It is clear that our data are so precise that they reproduce the theoretically-predicted downward deviation of Δ_π from the BCS-like behaviour. However, the actual shape of the curve does not correspond to the theoretical one, maybe indicating that, in our samples, the values of some parameters are slightly different from those used in the model.

It is clear that the whole procedure described so far (that gave one of the clearest direct evidences of the existence of two distinct gaps in MgB_2 up to T_c [9]) is based on the disappearance of the π-band contribution to the conductance in a field of about 1 Tesla. To obtain the whole magnetic-field dependence of the gaps, we measured the conductance curves of Ag-paint, *ab*-plane contacts at $T = 4.2$ K, in the presence of a magnetic field of increasing intensity applied parallel to the *c* axis. An example of the results is shown in Figure 2a (symbols). The solid lines in the same graph are the best-fitting curves of the form $\sigma(B) = w_\pi\sigma_\pi(B) + (1-w_\pi)\sigma_\sigma(B)$, where w_π is assumed to be field-independent. Above 1 Tesla the best fit is obtained by keeping $\sigma_\pi(B) = 1$ (for details on the fitting procedure see Ref. [18]). The values of the gaps are shown in Figure 2b as solid symbols. For comparison, superimposed to the experimental $\Delta_{\sigma,\pi}(B)$ curves we report also the theoretically-predicted values of the maximum order parameter (calculated at the boundary of the vortex-lattice unit cell [19]) in the case where the π-band diffusivity D_π is 5 times greater than D_σ. The comparison is only qualitative, since PCS rather measures an average of the pair potential in different regions of the vortex lattice, but the agreement is surprising. This indicates that, even in best-quality single crystals, the π band is in the moderate dirty limit [*], in agreement with the results of STM [20] and de Haas-van Alphen measurements [21].

In the case of Figure 2 the junction featured very good curves, but broke down before the normal state was reached. In many other cases we were able to follow the evolution of the conductance curves up to the critical field [18], here defined as the field that marks the return to the normal-state conductance. Because of the anisotropy of MgB_2, the values of the critical field depends very much on whether $\mathbf{B} \parallel ab$ or $\mathbf{B} \parallel c$. The resulting values

[*] In this context, the expression "clean" and "dirty" refer to *intraband* scattering. According to Anderson's theorem, this scattering cannot reduce the critical temperature of the compound nor the amplitude of the gaps.

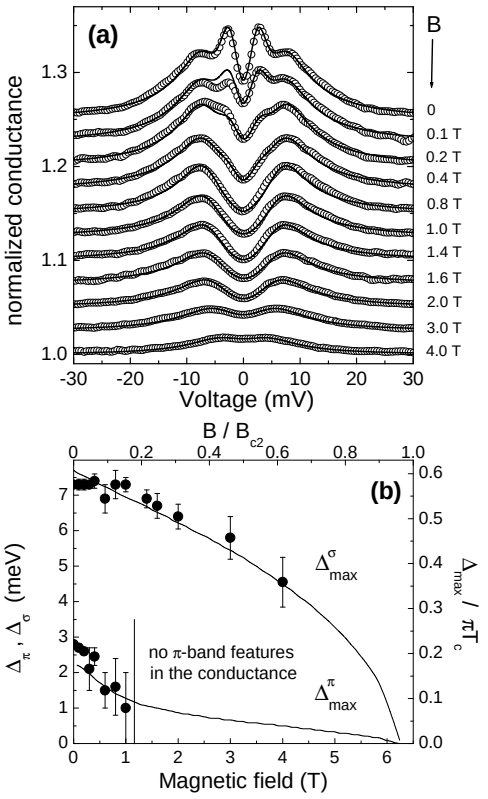

Figure 2. (a) Normalized conductance curves of a Ag-paint, *ab*-plane junction, in magnetic fields of increasing intensity applied parallel to the *c* axis. Symbols:experimental data; Lines: best-fitting curves obtained with the two-band BTK model. (b) Symbols: magnetic field dependence of the gaps as determined from the fit of the curves in (a) (the scale is on the bottom and left axes). Lines: dependence of the maximum pair potential, calculated in Ref.[19] on the reduced field B/B_{c2} (the scale is on the top and right axes). The reported lines refer to the case where $D_\pi = 5D_\sigma$.

of the critical field B_{c2} are reported in Figure 3a as a function of the reduced temperature T/T_c. In the same figure, the shaded regions are lower-bounded by the values of the critical field given by bulk measurements (i.e. thermal conductivity [22], specific heat [23] and torque magnetometry [24]) and upper-bounded by the field that, at any temperature, marks the onset of the superconducting transition in the $\rho(B)$ curve [23, 25]. This field has been recently identified [23] with the surface critical field B_{c3} [26]. It is clearly seen that, in both the $\mathbf{B} \parallel c$ and $\mathbf{B} \parallel ab$ configurations, our values practically coincide with the bulk critical field at high temperatures, then approach the surface critical field at lower temperature and finally turn again toward the bulk values. The "crossover" from B_{c2} to nearly B_{c3} always occurs at $T/T_c \simeq 0.7$ and thus seems to be temperature-induced rather than field-induced. The more pronounced curvature of our data with respect to other results gives rise to a temperature dependence of the anisotropy ratio $\gamma = B_{c2}^{ab}/B_{c2}^{c}$ (solid circles in Figure 3b) which, at $T < 0.7\,T_c$, differs very much from that given by bulk techniques (open symbols). However, it is interesting to note that a similar $\gamma(T)$ behaviour was theoretically predicted and reported in Ref. [27] in the case where $D_\pi = 10D_\sigma$. Again, this indicates that – at least at the surface – our MgB_2 single crystals present a π band in the moderate dirty limit, in complete agreement with the results of Figure 2. Notice that this conclusion has a great fundamental importance since the role and the amount of intraband scattering in MgB_2 is still a matter of debate, and alternative models (for negligible [28] and non-negligible [19, 27] intraband scattering) have

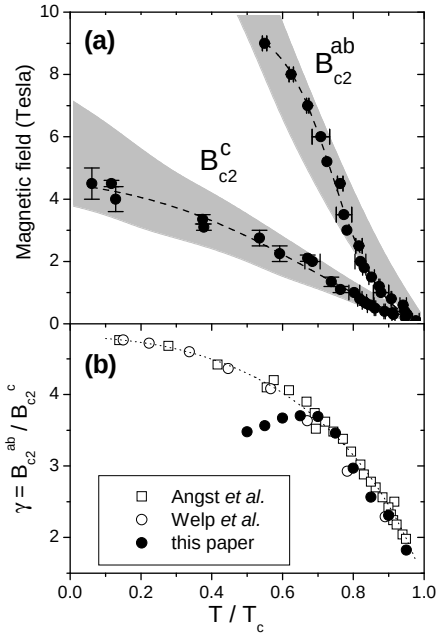

Figure 3. (a) Temperature dependence of the critical field of MgB_2, both for **B** $\|$ *ab* and **B** $\|$ *c*. Symbols: experimental data obtained from PCS; the critical field is identified with the field that marks the return to the normal-state conductance. The gray regions are lower bounded by the values of B_{c2} given by bulk-sensitive techniques (specific heat [23], torque magnetometry [24], thermal conductivity [22]) and upper-bounded by the values measured by transport (onset) [23, 25]. (b) Temperature dependence of the anisotropy $\gamma = B_{c2}^{ab}/B_{c2}^{c}$ measured in similar single crystals by different techniques: torque magnetometry (□), specific heat (○), and PCS (●).

been proposed to explain experimental findings in this compound.

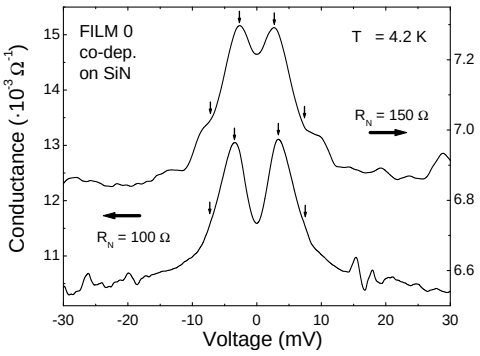

Figure 4. Two examples of as-measured (i.e., non-normalized) conductance curves of In point contacts on MgB_2 films grown on SiN amorphous substrate. The curves were measured in liquid helium. Also indicated are the positions of the conductance maxima and of the shoulders related to the energy gaps.

3.2. PCS in thin films

Figure 4 reports the conductance curves of two In/MgB_2 point contacts made on the surface of a thin film ("FILM 0") grown on silicon nitride by co-deposition of Mg and B and subsequent *in situ* annealing. The resistive critical temperature of the film is $T_c = 36$ K , and the transition is very sharp ($\Delta T_c \leq 1$ K). The normal-state resistance of the contacts is also indicated. The conductance curves feature clear maxima, related to the small gap, at ± 2.6 mV (upper curve) and ± 3.4 mV (lower curve). A shoulder at about ± 7.2 mV is clearly seen in the upper curve, but is also present (even if smoother) in the lower one. Comparing the curves to those obtained in single crystals (see Figure 1) it is clear that their shape is compatible with a *preferential c*-axis orientation of the films. However, the rather evident contribution of the σ band (especially in the upper curve) indicates that this orientation is not complete.

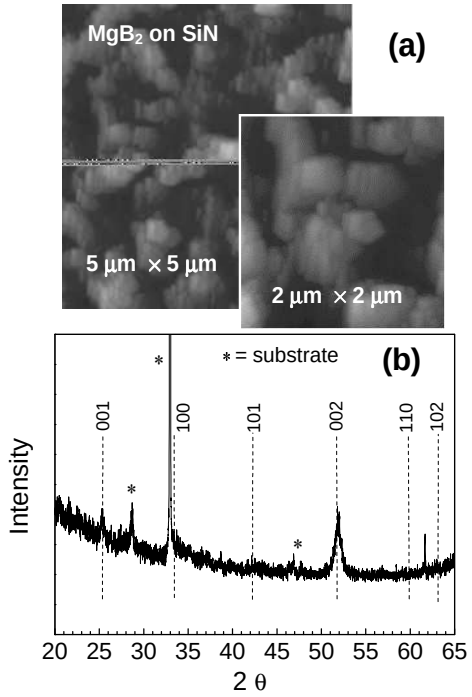

Figure 5. (a) AFM images of a MgB_2 film grown on amorphous silicon nitride. The presence of plate-like grains, with *c* axis either parallel or perpendicular to the film surface, is clearly seen. (b) X-ray diffraction spectrum of the same film. The clear [001] and [002] peaks, together with the absence of the other reflections indicated, shows a preferential *c*-axis orientation.

The AFM images of the film surface reported in Figure 5a clarify this point. The main image and its enlargement (inset) clearly show vertically- and horizontally-packed plate-like grains, that in PCS measurements behave as a set of crystals in which the current is injected along to the *c* axis or along the *ab* planes. This explains not only the shape of the curves, with the excess of *ab*-plane contribution, but also its variability from point to point. An analysis of the images reported in Figure 5a gives the average grain size ($200 \div 250$ nm) and the RMS roughness, that in this case is about 30 nm (even if values down to 10 nm were obtained). The small roughness is particularly important in view of the fabrication of planar Josephson junctions, where the control of the interface smoothness is crucial. The XRD spectrum reported in Figure 5b shows clear (001) and (002) diffraction maxima, coming from the *c*-axis oriented main phase, whose intensity is however smaller than in single crystals. The absence of a clear (101) reflection, that is the most intense in powders, indicates that most of the film is oriented, in spite of the amorphous SiN substrate. A very intense spurious peak

due to the crystalline Si substrate (on which SiN is deposited) is also shown.

In addition to the information on the orientation, two other important indications can be extracted from the Andreev-reflection spectra reported in Figure 4. First, the possibility to observe Andreev reflection by PCS means that the contact is S-N, i.e. the potential barrier Z at the interface is very small [16]. In other words, there cannot be any insulating layer (for example, of MgO due to the reaction with air) covering the surface ♯. This finding is consistent with the remarkable durability of these films that, if kept in suitably dry atmosphere, retain their properties for several months. The second important indication concerns the "clean" or 'dirty" limit conditions at the surface of the film. In this context, the expressions "clean" and "dirty" are referred to the *interband* scattering. According to the two-band model appeared in literature [3], if the interband scattering is sufficiently strong, the critical temperature falls drastically and the two gaps merge in one single isotropic gap $\Delta_{\rm dirty}$, with BCS-like temperature dependence and zero-temperature value $\Delta_{\rm dirty} \simeq 4.2$ meV. It is clear that the evidence of two distinct gaps in the curves of Figure 4 indicates that the surface of the films is in clean limit, even if this kind of measurements cannot provide a measure of the scattering rate.

Figure 6a reports the conductance curves of a Ag-paint spot contact on a 100 nm-thick MgB_2 film grown on *c*-cut sapphire by PLD and then annealed *ex situ* in Mg vapour ("FILM 1" in Refs.[11, 29]). The critical temperature of the film, measured by transport, is $T_{\rm c} = 29.5$ K, with $\Delta T_{\rm c} = 2$ K. The strong *c*-axis orientation of the film is witnessed both by the XRD spectrum reported in Figure 6b (note that the (101) peak, that is the most intense in powders, is absent) and by the large values of the low-temperature anisotropy ($\gamma = 3.0$), one of the highest reported in literature for films. The film also features in-plane orientation, with a 30°-tilt with respect to the substrate, as shown by Φ-scan measurements [11]; other characteristics are reported in Ref.[29]. The conductance curve of Figure 6a shows maxima at ± 4.5 mV and no clear shoulders. The absence of multigap features and the position of the maxima suggests that the measured gap is very likely to be $\Delta_{\rm dirty}$. Since in the dirty limit the material becomes isotropic, it is clear that, in this case, PCS is unable to give any information about the orientation of the film. However, it provides a direct evidence of the degradation of the material, e.g. due to the exposition to air and moisture. This degradation is definitely restricted to the very top layer of the film (in fact, transport measurements gave reproducible values of the critical field [29] even if repeated after several months) and is thus difficult or even impossible to detect with bulk-sensitive techniques. In this sense, PCS has the unique capability to probe the conditions of the surface, that is particularly useful in view of the fabrication of planar Josephson junctions, where the control of the interface is crucial.

Figure 7a reports the conductance curve of a Ag-paint contact on a MgB_2 film grown on MgO (111) substrate ("FILM 2" in Ref.[29]). The critical temperature of the film is a little higher than that of FILM 1, i.e. $T_{\rm c} = 32$ K with $\Delta T_{\rm c} = 1.5$ K. As shown by the XRD spectrum reported in Figure 7b, the film is strongly *c*-oriented, even if it does not feature in-plane orientation. The shape of the conductance curve clearly denotes that the contact is in the "tunnelling" regime (large Z) rather than in the Andreev-reflection regime (small Z). As in the case of Figure 6a, the curve in Fig. 7a presents conductance maxima at energies (± 4.2 meV) that correspond to the gap in dirty limit, $\Delta_{\rm dirty}$. In this case, however, additional features are present in the form of shoulders at ± 2.7 meV, that should correspond to the small gap Δ_π. This result can be explained by admitting that parallel microcontacts are established between the Ag glue and the film, in regions of the film where the surface is clean (and thus Δ_π is observed) and dirty (where $\Delta_{\rm dirty}$ is measured). In principle, the absence of any clear evidence of Δ_σ in the conductance curves could be interpreted as a further indication of good *c*-axis orientation of the clean material; however, in the present case the measure is probably too noisy and broadened for this conclusion to be definitely drawn.

As in the previous case, the observation of $\Delta_{\rm dirty}$ in some regions of the contact speaks in favour of aging effects, that cannot be excluded due to the rather long time elapsed between the film deposition and the PCS measurements (several months). Further support to this hypothesis comes from the fact that we could never observe Andreev reflection in contacts made on this films. In other words, we always obtained S-I-N contacts, with a non-negligible

♯ Notice that this conclusion can be drawn here because the contact is "soft". On the contrary, in the conventional technique the tip can damage and even perforate the surface layer and this information is lost.

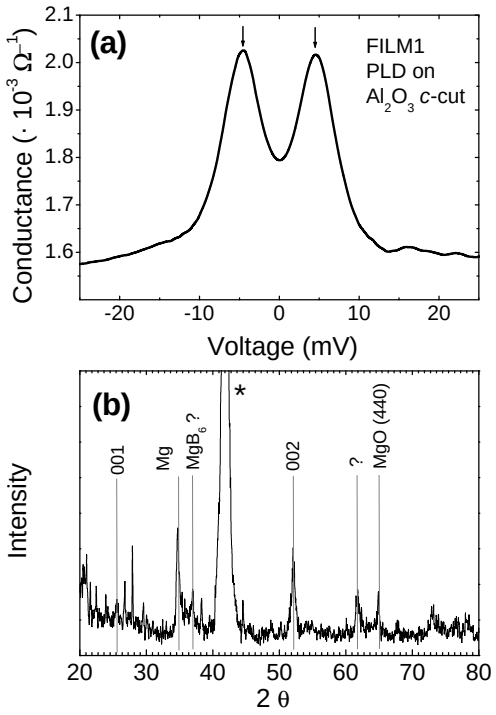

Figure 6. (a) Non-normalized experimental conductance curve of a Ag-paint contact on a MgB_2 thin film produced by PLD from stoichiometric target on *c*-cut sapphire and subsequent *ex situ* annealing ("FILM 1" in Refs. [11, 29]). Arrows indicate the position of the conductance maxima. (b) X-ray diffraction spectrum of the same film, from Ref. [11]. Only the $(00l)$ reflections are evident for the MgB_2 phase, meaning that this phase is *c*-axis oriented. Note the presence of a spurious MgO phase, maybe related to the degradation of the surface observed by PCS.

potential barrier at the interface, and with tunnelling-like characteristics. This is probably due to the presence of an oxide layer on the top of the film – i.e. MgO due to the exposition to air and moisture – acting as an insulating barrier and preventing the direct contact between the superconductor and the normal metal. As a matter of fact, some peaks due to MgO are often found in the XRD spectra, as in Figure 6 (in the case of FILM 2, however, they are not conclusive since the substrate is made of MgO too). It is worth noting that, again, no evidence of this surface degradation was found in critical field measurements, that always gave a very high value of the anisotropy ($\gamma = 3.5$) supporting the spectroscopic evidence of *c*-axis orientation.

4. Conclusions

In conclusion, we have shown that "soft" PCS, that employs small In spots or Ag-paste drops to make the "point" contacts, presents unique advantages for the investigation of the fundamental superconducting properties of MgB_2 as well as for the characterization of the morphological and electronic properties of crystal and film surfaces. It is clear that these advantages hold for any superconductor, provided that its surface is sufficiently clean, stable in air, metallic and homogeneous to obtain clear Andreev-reflection curves. Morever, some of these requirements are not really strict. For example, even in the presence of an insulating surface layer (either intentionally grown or consequent to degradation) this technique permits the creation of useful weak-link SIN junctions (as shown in Figure 7).

In particular, with respect to standard PCS – where a metallic tip is pressed against the

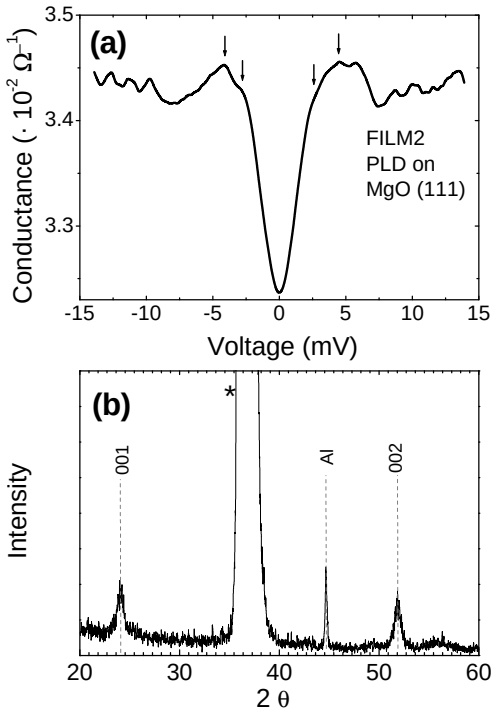

Figure 7. (a) Non-normalized experimental conductance curve of a Ag-paint contact on a MgB_2 thin film produced by PLD on MgO (111) and *ex situ* annealing. Arrows indicate the position of the conductance maxima and of the shoulders related to energy gaps. (b) X-ray diffraction spectrum of the same film, showing clear (001) and (002) reflections. The absence of the (101) peak was verified by tilting the sample by about 0.5° to avoid the superposition with the substrate peak. The film is *c*-axis oriented but features no in-plane orientation.

sample surface – our "soft" PCS technique ensures: i) greater stability and reproducibility of the junctions at the change of temperature and magnetic field; ii) absence of damage or perforation of the surface, that prevents unwanted contributions from the underlying bulk material; iii) greater control of the directionality of the contact, that can be essential in the study of anisotropic superconductors like MgB_2. On the other hand, the smaller area of the contact usually obtained by metallic tips can be useful in the study of superconductors with non-homogeneous or granular surfaces. In this respect, a further improvement of the technique with a reduction of the minimum apparent contact area is under study.

This work was done within the project PRA "UMBRA" of INFM, the ASI contract N. I/R/109/02 and the INTAS project N. 01-0617. V.A.S. acknowledges the support from RFBR (project N. 02-02-17133) and the Ministry of Science and Technologies of the Russian Federation (contract N. 40.012.1.1.1357).

References

[1] Nagamatsu J, Nakagawa N, Muranaka T, Zenitani Y and Akimitsu J 2001 *Nature* **410** 63.
[2] Liu A Y, Mazin I I and Kortus J 2001 *Phys. Rev. Lett.* **87** 87005.
[3] Brinkman A, Golubov A A, Rogalla H, Dolgov O V, Kortus J, Kong Y, Jepsen O and Andersen O K 2001 *Phys. Rev.* B **65** 180517(R).
[4] Choi H J, Roundy D, Sun H, Cohen M L and Louie S G 2001 *Nature* **418** 758.
[5] Gonnelli R S, Calzolari A. Daghero D, Ummarino G A, Stepanov V A, Giunchi G, Ceresara S and Ripamonti G 2001 *Phys. Rev. Lett* **87** 097001.
[6] Burnell G, Kang D -J, Lee H N, Moon S H, Oh B and Blamire M G 2001 *Appl. Phys. Lett.* **79** 3464; Carapella G, Martucciello N, Costabile G, Ferdeghini C, Ferrando V and Grassano G 2002 *Appl. Phys. Lett.* **80** 2949;

Mijatovic D, Brinkman A, Oomen I, Rijnders G, Hilgenkamp H, Rogalla H and Blank D H A 2001 *Appl. Phys. Lett.* **80** 2141.
[7] Zhang Y, Kinion D, Chen J, Clarke J, Hinks D G and Crabtree G W 2001 *Appl. Phys. Lett.* **79** 3995; Burnell G, Kang D -J, Ansell D A, Lee H N, Moon S H, Oh B, Tarte E J and Blamire M G 2003 *Supercond. Sci. Technol.* **16** 254; Brinkman A, Veldhuis D, Mijatovic D, Rijnders G, Blank D H A, Hilgenkamp H and Rogalla H 2001 *Appl. Phys. Lett.* **79** 2420.
[8] Szabó P, Samely P, Kačmarčík J, Klein T, Marcus J, Fruchart D, Miraglia S, Marcenat C and Jansen A G M 2001 *Phys. Rev. Lett.* **87** 137005.
[9] Gonnelli R S, Daghero D, Ummarino G A, Stepanov V A, Jun J, Kazakov S M and Karpinski J 2002 *Phys. Rev. Lett.* **89** 247004.
[10] Karpinski J, Angst M, Jun J, Kazakov S M, Puzniak R, Wisniewski A, Roos J, Keller H, Perucchi A, Degiorgi L, Eskildsen M R, Bordet P, Vinnikov L and Mironov A 2003 *Supercond. Sci. Technol.* **16** 221; Karpinski J, Kazakov S M, Jun J, Angst M, Puzniak R, Wisniewski A and Bordet P 2003 *Physica C* **385** 42.
[11] Ferrando V, Amoruso S, Bellingeri E, Bruzzese R, Manfrinetti P, Marrè D, Velotta R, Wang X and Ferdeghini C 2003 *Supercond. Sci. Technol.* **16** 241.
[12] Monticone E, Gandini C, Portesi C, Rajteri M, Bodoardo S, Penazzi N, Dellarocca V and Gonnelli R 2003 *Appl. Phys. Lett.*, submitted.
[13] Kashiwaya S and Tanaka Y 2000 *Rep. Prog. Phys.* **63** 1641.
[14] Zeng X H *et al* 2002 *Nature Materials***1** 35-38.
[15] Bugoslavsky Y, Miyoshi Y, Perkins G K, Caplin A D, Cohen L F, Pogrebnyakov A V and Xi X X 2003 *Preprint* cond-mat/0307540.
[16] Blonder G E, Tinkham M and Klapwijk T M 1982 *Phys. Rev. B* **25** 4515.
[17] Gonnelli R S, Daghero D, Ummarino G A, Stepanov V A, Jun J, Kazakov S M and Karpinski J 2003 *Physica C* **385** 255-263.
[18] Gonnelli R S, Daghero D, Calzolari A, Ummarino G A, Dellarocca V, Stepanov V A, Jun J, Kazakov S M and Karpinski J, 2003 *Preprint* cond-mat/0308152, submitted to *Phys. Rev. Lett.*
[19] Koshelev A E and Golubov A A 2003 *Phys. Rev. Lett.* **90** 177002.
[20] Eskildsen M R, Kugler M, Tanaka S, Jun J, Kazakov S M, Karpinski J and Fischer Ø2002 *Phys. Rev. Lett.* **89** 197003.
[21] Carrington A, Meeson P J, Cooper J R, Balicas L, Hussey N E, Yelland E A, Lee S, Yamamoto A, Tajima S, Kazakov S M and Karpinski J 2003 *Phys. Rev. Lett.* **91** 037003.
[22] Sologubenko A V, Jun J, Kazakov S M, Karpinski J and Ott H R 2002 *Phys. Rev.* B **65** 180505(R).
[23] Welp U *et al.* 2003 *Physica C* **385** 154.
[24] Angst M, Puzniac R, Wisniewski A, Jun J, Kazakov S M, Karpinski J, Roos J and Keller H 2002 *Phys. Rev. Lett.* **88** 167004.
[25] Eltsev Yu 2003 *Physica C* **385** 162.
[26] D. Saint-James and P. G. De Gennes, Physics Letters **7**, 306 (1963).
[27] Gurevich A 2003 *Phys. Rev. B* **67** 184515.
[28] Dahm T and Schopohl N 2003 *Phys. Rev. Lett.***91** 017001; Dahm T, Graser S and Schopol N 2003 *Preprint* cond-mat/0304194.
[29] Ferrando V, Manfrinetti P, Marrè D, Putti M, Sheikin I, Tarantini C and Ferdeghini C 2003 *Preprint* cond-mat/0307013.